# *Articles*

## Reactivity of Silica-Supported Hafnium Tris-neopentyl with Dihydrogen: Formation and Characterization of Silica Surface Hafnium Hydrides and Alkyl Hydride

Géraldine Tosin, Catherine C. Santini,* Anne Baudouin, Aimery De Mallman, Steven Fiddy,† Céline Dablemont, and Jean-Marie Basset*

*C2P2, Laboratoire de Chimie OrganoMétallique de Surface (LCOMS), UMR 5265 CNRS-CPE Lyon, 43, Boulevard du 11 Novembre 1918, 69616 Villeurbanne, Cedex, France*

*Received March 7, 2007*

Surface organometallic chemistry represents an approach to the preparation of well-defined single sites for catalysis, the possibility of observing some elementary reaction steps, and the development of a fundamental basis for the synthesis of tailor-made catalysts. Silica-supported metal hydrides are an important class of new catalysts for alkane metathesis, methanolysis of alkanes, Ziegler−Natta depolymerization, alkane hydrogenolysis, etc. Understanding their mechanism of formation and aging is crucial. In the work presented here, the reaction of the well-defined silica surface organometallic complex $[(\equiv SiO)Hf(CH_2tBu)_3]$, **1**, ($(\equiv SiO)$ = silica surface ligand) with dihydrogen has been performed at different temperatures ($\theta$). At $\theta \leq 100$ °C, there is formation of a stable hafnium neopentyl dihydride, $[(\equiv SiO)Hf(CH_2tBu)(H)_2]$, **2**. For $100 \leq \theta \leq 200$ °C, **2** affords, via a succession of $\beta$-methyl transfer and subsequent hydrogenolysis of the resulting Hf−alkyl bonds, the formation of $[(\equiv SiO)_2Hf(H)_2]$, **3**, and $[(\equiv SiO)_3SiH]$ with evolution of methane ($C_1$) and ethane ($C_2$). For $150 \leq \theta \leq 300$ °C, **3** is totally converted into $[(\equiv SiO)_3Hf(H)]$, **4**, and $[(\equiv SiO)_2Si(H)_2]$. For $\theta \geq 300$ °C, $[(\equiv SiO)_3Hf(H)]$, **4**, is transformed into $[(\equiv SiO)_4Hf]$, **5**, and $[(\equiv SiO)_2Si(H)_2]$ into $[(\equiv SiO)_3SiH]$. At this temperature, $[(\equiv SiO)_3SiH]$ is the only hydride remaining on the surface. All these species have been characterized with a multitude of techniques such as elemental analysis and infrared, $^1H$ solid-state NMR, $^1H$ DQ solid-state NMR, and EXAFS spectroscopies. The results elucidate a complete mechanism of surface organometallic chemistry by which one observes the stepwise transformation of a hafnium tris-neopentyl to hafnium neopentyl hydrides, hafnium mono- and bis-hydrides, silicon bis-hydride with the ultimate formation of tetrasiloxy surface species $[(\equiv SiO)_4Hf)]$, and silicon mono-hydride, the only hydride stable at very high temperature. It is suggested that the formation of these surface silicon hydrides is responsible for the aging of such catalysts in any reaction involving dihydrogen.

### Introduction

Surface organometallic chemistry represents an approach to the preparation of well-defined active sites for catalysis, the possibility of observing some elementary reaction steps, and the development of a fundamental basis for the synthesis of tailor-made catalysts.[1] Access to "single-site" systems for catalysis, and especially for alkane transformation, is the main objective of this approach. The first step for the synthesis of tailor-made catalysts generally used in our laboratory[1−4] consists of the reaction of alkyl complexes $MR_n$ with semihydroxylated oxide surfaces. This affords well-defined "monosiloxy" surface complexes, which are the starting entity to generate new surface complexes linked to silica through two or three siloxy bonds. Unfortunately, once the complex is grafted via one siloxy ligand (arising from the first reactive silanols), the formation of several bonds between the transition metal and the surface is so far not fully elucidated.

In the case of zirconium supported on silica the starting complex $[(\equiv SiO)Zr(CH_2tBu)_3]$ leads under hydrogen treatment to a mixture of zirconium mono- and bis-hydrides $[(\equiv SiO)_3Zr(H)]$ (70−80%) and $[(\equiv SiO)_2Zr(H)_2]$ (20−30%), along with silicon

* Corresponding authors. Fax: 04 72 43 17 95. E-mail: santini@cpe.fr; basset@cpe.fr.

† Present address: SRS of the CCLRC, Daresbury, UK

(1) (a) Zakharov, V. A.; Yermakov, Yu. I. *Catal. Rev. Sci. Eng.* **1979**, *19*, 67−103. (b) Ryndin, Yu. A.; Yermakov, Yu. I. *Surface Organometallic Chemistry, Molecular Approaches to Surface Catalysis*; Basset, J. M., Ed.; NATO ASI Series, Series C; 1988; Vol. 23, pp 127−41. (c) Basset, J.-M.; Choplin, A. *J. Mol. Catal.* **1983**, *21*, 95−108. (d) Scott, S. L.; Basset, J.-M.; Niccolai, G. P.; Santini, C. C.; Candy, J.-P.; Lecuyer, C.; Quignard, F.; Choplin, A. *New J. Chem.* **1994**, *18*, 115−22. (e) Basset, J.-M.; Lefebvre, F.; Santini, C. C. *Coord. Chem. Rev.* **1998**, *178−180*, 1703−1723. (f) Copéret, C.; Chabanas, M.; Saint-Arroman, R. P.; Basset, J.-M. *Angew. Chem., Int. Ed.* **2003**, *42*, 156−181. (f) Quignard, F.; Choplin, A. *Comprehensive Coordination Chemistry II*; Pergamon: Oxford, 2004; Vol. 9, pp 445−470.

(2) Lecuyer, C.; Quignard, F.; Choplin, A.; Olivier, D.; Basset, J.-M. *Angew. Chem., Int. Ed.* **1991**, *30*, 1660−1661.

(3) Quignard, F.; Choplin, A.; Basset, J.-M. *Chem. Commun.* **1991**, 1589−1590.

(4) Corker, J.; Lefebvre, F.; Lecuyer, C.; Dufaud, V.; Quignard, F.; Choplin, A.; Evans, J.; Basset, J.-M. *Science* **1996**, *271*, 966−969.

10.1021/om070214q CCC: $37.00 
Publication on Web 07/11/2007

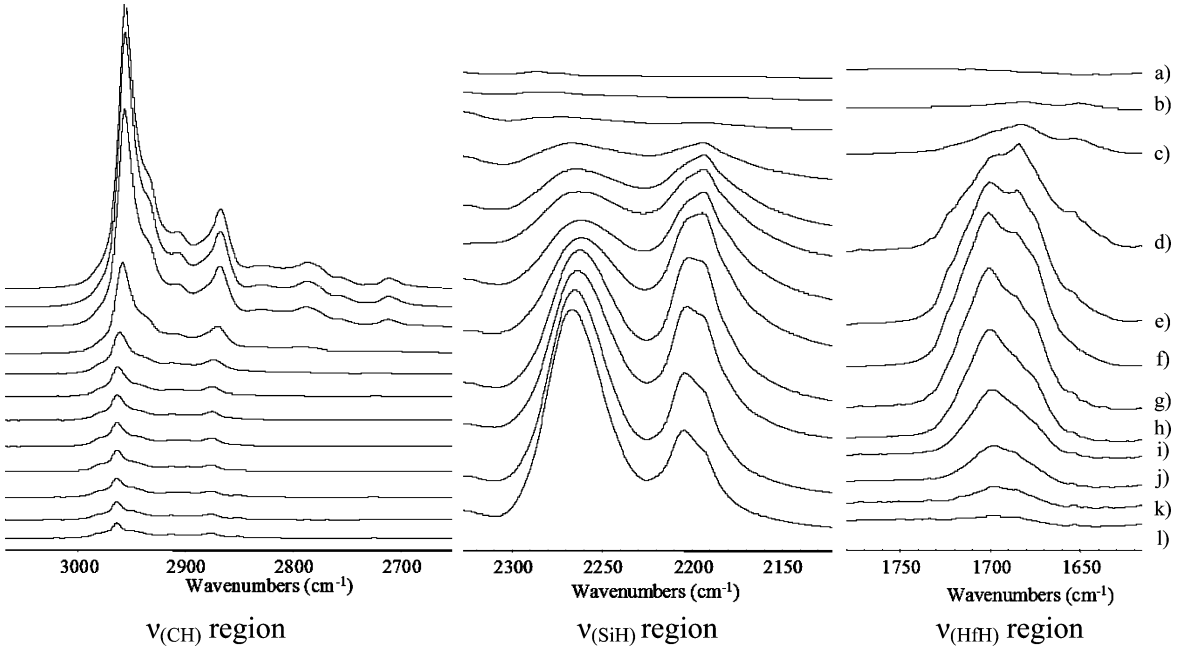


**Figure 1.** Hydrogenolysis of **1** monitored by in situ IR spectroscopy: (a) 25 °C; (b) 75 °C, 4 h; (c) 75 °C, 16 h; (d) 100 °C, 4 h; (e) 150 °C, 4 h; (f) 150 °C, 20 h; (g) 200 °C, 4 h; (h) 250 °C, 4 h; (i) 300 °C, 4 h; (j) 350 °C, 4 h; (k) 400 °C, 4 h; (l) 450 °C, 4 h.

mono- and bis-hydrides: $[(\equiv SiO)_3SiH]$ and $[(\equiv SiO)_2SiH_2]$.[2−7] These surface hydrides have been fully characterized by infrared spectroscopy, EXAFS, GC analysis, and solid-state NMR spectroscopy ($^1H$ and double-quanta (DQ) proton).[8] Unfortunately in the case of zirconium, the chemistry is not simple and no systematic study has been performed to understand how these hydrides are really formed on a partially dehydroxylated surface.

These zirconium hydrides are active under mild conditions in Ziegler−Natta polymerization,[5,9,10] hydrogenolysis of polyethylene and polypropylene,[11,12] alkane isomerization, hydrogenolysis of alkanes,[3,13−15] hydrogenation of olefins and benzene,[5,9,10,16] and isotopic exchanges in alkanes.[17]

In contrast, surface hydrides of hafnium have been much less studied in terms of catalytic performance. They have only been reported as intermediates in catalytic reactions, and there is no full characterization or information about their mechanism of formation or their mechanism of aging in catalytic reactions involving dihydrogen as a reagent.[5,9,10,18]

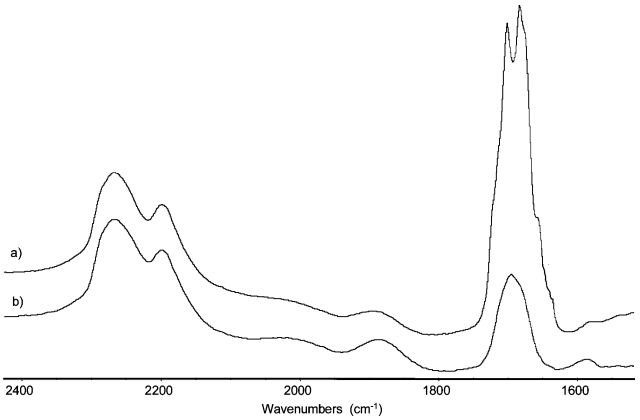


**Figure 2.** Deuterium exchange monitored by in situ IR spectroscopy. Enlargement of the 2400−1600 $cm^{-1}$ spectral regions: (a) **1** after treatment under $H_2$ (100 °C); (b) after treatment under $D_2$ at 25 °C for 2 h.

Recently, we have reported that the reaction of tetraneopentylhafnium $[Hf(CH_2tBu)_4]$ with silica surface treated at 800 °C, $SiO_{2-(800)}$, affords a single-site surface complex, $[(\equiv SiO)Hf(CH_2tBu)_3]$, **1**,[19,20] which is more stable,[19,20] less reducible under hydrogen atmosphere,[21−23] and more active in alkane hydrogenolysis than surface zirconium analogues.[18]

The objective of this study is to characterize the surface hydrides resulting from the hydrogenolysis of **1** and to obtain information on the mechanism of their formation.

## Results

The reaction of $[(\equiv SiO)Hf(CH_2tBu)_3]$, **1**, with dihydrogen has been monitored by infrared spectroscopy at different temperatures, in a batch system with analysis of any evolved gas. This reaction was also monitored through temperature programmed reactor (TPR) experiments, which were performed in a continuous-flow reactor at 75 and 150 °C with in situ analysis of any evolved gas. The silica support is Flame Aerosil silica from Degussa. It is always pretreated at 800 °C under vacuum and further referred to as $SiO_{2-(800)}$.

(5) Zakharov, V. A.; Dudchenko, V. K.; Paukstis, E.; Karakchiev, L. G.; Ermakov, Y. I. *J. Mol. Catal.* **1977**, *2*, 421−435.
(6) Pyle, A. M.; Jens, K. J. *J. Mol. Catal.* **1986**, *38*, 337.
(7) Vasnestov, S. A.; Nosov, V. A.; Mastikhin, V. M.; Zakharov, V. A. *J. Mol. Catal.* **1989**, *53*, 37.
(8) Rataboul, F.; Baudouin, A.; Thieuleux, C.; Veyre, L.; Coperet, C.; Thivolle-Cazat, J.; Basset, J.-M.; Lesage, A.; Emsley, L. *J. Am. Chem. Soc.* **2004**, *126*, 12541−12550. Avenier, P.; Lesage, A.; Taoufik, M.; Baudouin, A.; De Mallmann, A.; Fiddy, S.; Vautier, M.; Veyre, L.; Basset, J.-M.; Emsley, L.; Quadrelli, E., *J. Am. Chem. Soc.* **2007**, *129*, 176−186.
(9) Zakharov, V. A.; Yermakov, Y. I. *Catal. Rev.* **1979**, *19*, 67−103.
(10) Zakharov, V. A.; Ryndin, Y. A. *J. Mol. Catal.* **1989**, *56*, 183−193.
(11) Dufaud, V.; Basset, J.-M. *Angew. Chem., Int. Ed.* **1998**, *37*, 806−810.
(12) Thieuleux, C.; Quadrelli, E. A.; Basset, J.-M.; Doebler, J.; Sauer, J. *Chem. Commun.* **2004**, 1729−1731.
(13) Quignard, F.; Lecuyer, C.; Bougault, C.; Lefebvre, F.; Choplin, A.; Olivier, D.; Basset, J.-M. *Inorg. Chem.* **1992**, *31*, 928−930.
(14) Quignard, F.; Lecuyer, C.; Choplin, A.; Olivier, D.; Basset, J.-M. *J. Mol. Catal.* **1992**, *74*, 353−363.
(15) Vidal, V.; Theolier, A.; Thivolle-Cazat, J.; Basset, J.-M.; Corker, J. *J. Am. Chem. Soc.* **1996**, *118*, 4595−4602.
(16) Schwartz, J.; Ward, M. D. *J. Mol. Catal.* **1980**, *8*, 465−469.
(17) Casty, G. L.; Matturro, M. G.; Myers, G. R.; Reynolds, R. P.; Hall, R. B. *Organometallics* **2001**, *20*, 2246−2249.
(18) d'Ornelas, L.; Reyes, S.; Quignard, F.; Choplin, A.; Basset, J.-M. *Chem. Lett.* **1993**, 1931−1934.

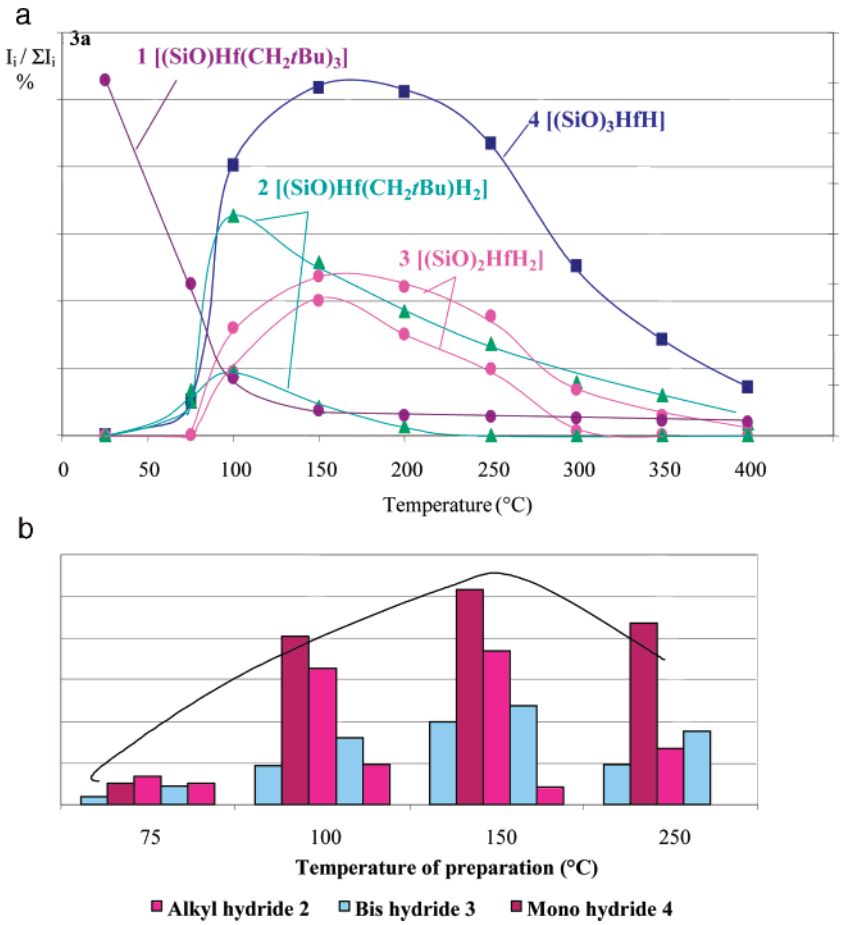


**Figure 3.** (a) Evolution of the intensity of the $\nu_{(HfH)}$ bands (left axis) and the $\nu_{(CH)}$ bands (right axis) versus temperature (● for **1**, ▲ for **2**, ● for **3**, ■ for **4**). Ordinates are intensities in arbitrary units. (b) Integration of intensity the $\nu_{(HfH)}$ peaks. Peak deconvolution of the various $\nu_{(HfH)}$ vibrations when these hydrides are prepared at different temperatures (**2** in red, **3** in blue, and **4** in brown). Ordinates are intensities in arbitrary units.

**In Situ IR Spectroscopy.** A silica pellet of [(≡SiO)Hf-($CH_2tBu)_3$], **1**, is heated under hydrogen (500 Torr) from 25 to 450 °C, with stepwise temperature increments of 25 °C, resting for at least 4 h at each temperature. The reaction is monitored by in situ FT infrared spectroscopy. The evolution of the different spectra in the $\nu_{(CH)}$, $\nu_{(HfH)}$, and $\nu_{(SiH)}$ regions versus temperature is depicted in Figures 1, 3, and 4.

Up to 75 °C, there are few changes in the spectra, indicating a higher thermal stability of **1** compared to [(≡SiO)Zr-($CH_2tBu)_3$]. From 75 to 150 °C, the intensity of the peaks due to the $\nu_{(CH)}$ and $\delta_{(CH)}$ vibrations of the neopentyl ligands of **1**, at respectively 3000−2500 $cm^{-1}$ and 1800−1300 $cm^{-1}$, decreases sharply to roughly 10 ± 5% of its initial value, then decreases slightly to remain steady at a value of ca. 5 ± 5% up to 450 °C (Figures 1 and 3). There is concomitant evolution of methane and ethane in the gas phase, a result that is observed in any hydrogenolysis reaction of group IV supported neopentyl complexes.[2,8,18]

From 75 °C, there is a progressive appearance of a complex pattern of several bands centered at 1700 $cm^{-1}$. All the bands of this pattern are affected in shape and intensity by the thermal changes. The total intensity of these bands is the highest at 150 °C and then decreases to zero at 400 °C (Figures 1 and 3). The intensity of this pattern of bands also decreases (by 70%) when the pellet is treated under dry $D_2$ (500 Torr) at room temperature (Figure 2), showing that these bands correspond to easily exchangeable hydrides.

This pattern of bands is thus attributed to the $\nu_{(HfH)}$ vibrations[10,24−30] of three main surface hafnium hydrides exchangeable with $D_2$ that we assign after deconvolution to three different hydrides: **2** [1651, 1685 $cm^{-1}$], **3** [1675, 1720 $cm^{-1}$], and **4** [1701 $cm^{-1}$] (see Supporting Information).

These bands behave differently upon heating: between 100 and 150 °C, the intensity of the peaks of **2** decreases sharply. The highest total intensity for the $\nu_{(HfH)}$ bands, ascribed to **3** and **4**, is obtained at 150 °C. Note that there is no change at all in the spectra when the pellet is kept at 150 °C during 20 h, suggesting that surface hydrides **3** and **4** are stable at this temperature. Above 150 °C, the intensity of all these bands decreases, but only those of species **4** remain present. Moreover, no new band appears, suggesting that no new Hf−H bond is formed. The fact that no Hf−H bond is present at 400 °C suggests that hafnium does not possess in its coordination sphere any other ligand but siloxy groups of silica and therefore suggests the formation of [(≡SiO)$_4$Hf], **5**. The global intensity

(19) (a) Tosin, G.; Santini, C. C.; Taoufik, M.; De Mallmann, A.; Basset, J.-M. *Organometallics* **2006**, *25*, 3324−3335. (b) Sharp, P. R.; Astruc, D.; Schrock, R. R. *J. Organomet. Chem.* **1979**, *182*, 477−88.
(20) Tosin, G.; Santini, C. C.; Taoufik, M.; Basset, J.-M. *Actual. Chim.* **2005**, *283*, 34−36.
(21) Besedin, D. V.; Ustynyuk, L. Y.; Ustynyuk, Y. A.; Lunin, V. V. *Mendeleev Commun.* **2002**, 173−175.
(22) Besedin, D. V.; Ustynyuk, L. Y.; Ustynyuk, Y. A.; Lunin, V. V. *Top. Catal.* **2005**, *32*, 47−60.
(23) Nesterov, G. A.; Zakharov, V. A.; Volkov, V. V.; Myakishev, K. G. *J. Mol. Catal.* **1986**, *36*, 253−269.

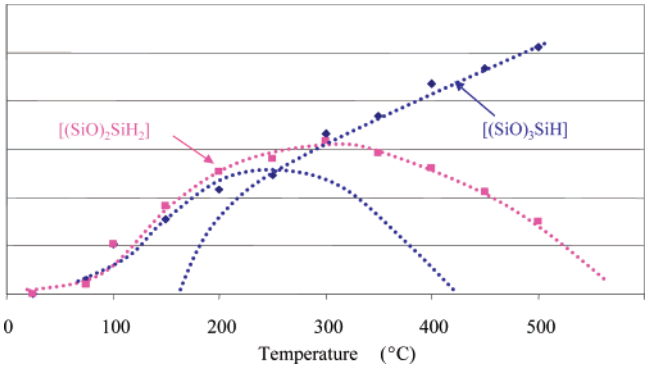


**Figure 4.** Evolution of the $\nu_{(SiH)}$ bands versus temperature (■ for $[(\equiv SiO)_2SiH_2]$ and ◆ for $[(\equiv SiO)_3SiH]$). Ordinates are intensities in arbitrary units.

of all the bands due to surface hydride hafnium is maximum at 150 °C, Figure 3b.

Whatever the temperature, the resolution of the pattern of peaks fits with the presence of the same three surface species, **2**−**4**: **2** [1651, 1685 $cm^{-1}$], **3** [1675, 1720 $cm^{-1}$], and **4** [1701 $cm^{-1}$]. Furthermore, when hydrogenolysis is performed at a fixed temperature ($\theta$ = 75, 125, 150, and 250 °C), the same pattern of peaks is obtained.

Above 100 °C, two broad bands also appear at 2264 and 2202 $cm^{-1}$ not exchangeable under $D_2$ attributed to $\nu_{(SiH)}$ and $\nu_{(SiH2)}$, respectively (Figure 1).[8,31,32] The intensity of the bands $\nu_{(SiH)}$ and $\nu_{(SiH2)}$ increases smoothly until 250 °C. At this temperature, $\nu_{(SiH2)}$ reaches a maximum then decreases to zero at 550−600 °C, while $\nu_{(SiH)}$ is still increasing up to 450 °C (Figure 4).

To conclude, this infrared study suggests that the hydrogenolysis reaction of **1** affords three surface hafnium hydrides: **2**, which is the first surface complex to be formed with a maximum just below 100 °C, then **3** and **4**, and above 250 °C $[(\equiv SiO)_4Hf]$, **5**. Up to 400 °C, only **5** and $[(\equiv SiH)]$ are present.

**Hydrogenolysis of 1 in a Continuous-Flow Reactor.** To attempt a further characterization of these surface hydrides and of their interconversion, hydrogenolysis of **1** was carried out in a continuous-flow reactor at 75 and 150 °C. The resulting solids are referred to as **1-$_{75}$** and **1-$_{150}$**, respectively.

Two different experiments were carried out following the same general protocol. **1** (ca. 300 mg) is introduced in a continuous-flow fixed-bed tubular reactor, and the flow rate of hydrogen is set to 3.1 mL·$min^{-1}$. After 200 min, the reactor is heated at a given temperature ($T$ = 75, 150 °C) with a temperature slope of 10 °C·$h^{-1}$. Gases evolved are continuously analyzed by gas chromatography. In each case, below 65 °C, only neopentane is detected. Above this temperature, methane and isobutane are formed concomitantly, followed by propane, and finally ethane appears. This sequence is the same for each experiment (see Supporting Information).

The hydrogenolysis of **1** at 75 °C, for 2800 min, leads to **1-$_{75}$**. During this reaction, the equivalent of 11 C/Hf (i.e., ca. 2 $CH_2tBu$ ligands) are evolved as alkanes (methane, $C_1$; ethane, $C_2$; propane, $C_3$; isobutane, $iC_4$; and neopentane, $neoC_5$), and the elemental analysis of **1-$_{75}$** indicates residual surface carbon with a C/Hf ratio of 5. During the hydrolysis of **1-$_{75}$**, alkanes (mainly neopentane) evolve. The C/Hf ratio of the residual solid (measured by elemental analysis) is equal to 1 (Figure 5). It is probable that some residual Hf−$CH_2tBu$ is still present in **1-$_{75}$**.

During the hydrogenolysis of **1** at 150 °C, for 2800 min, which affords the solid **1-$_{150}$**, the equivalent of 15 C/Hf are evolved as alkanes ($C_1$, $C_2$, $C_3$, $iC_4$, and $neoC_5$). The elemental analysis of **1-$_{150}$** indicates a C/Hf ratio smaller than 1. The hydrolysis of **1-$_{150}$** leads to the formation of traces of neopentane and methane, and no more carbon is detected by elemental analysis of the solid (Figure 5). Most likely, no Hf−$CH_2tBu$ ligand is present in **1-$_{150}$**.

**Solid-State NMR Spectroscopy of the Solids Obtained by Hydrogenolysis in a Batch Reactor.** Samples **1-$_\theta$** ($\theta$ = 75, 100, 125, 150, and 250 °C) were analyzed by solid-state NMR spectroscopy ($^1H$, $^{13}C$, and double-quanta (DQ) proton).

The $^1H$ NMR spectrum of each sample shows resonances in three different spectral domains: one band at 0.8 ppm; one asymmetric broad band at 4.5 ppm; and three resonances at 19, 25, and 32 ppm. The peaks at 0.8 and 4.5 pm are assigned respectively to the residual methyl groups of the *t*Bu fragments and to the Si−H groups (Figure 6).[31] The higher the temperature of hydrogenolysis, the smaller the intensity of the residual methyl group resonance and the higher the intensity of the Si−H resonance. The evolution of the intensity of the Si−H peak (4.4 ppm) with increasing temperature is parallel with those observed by infrared spectroscopy (Figure 4) (they increase in intensity up to 250 °C).

The intensity and presence of the signals at 19, 25, and 32 ppm varies with the temperature of reaction (Figure 6). They are attributed to the Hf−H resonance by analogy with the known resonance of molecular analogues, e.g., $Cp^*_2HfH_2$ $\delta_H$ = 15.6 ppm and $Cp^*_2Hf(OMe)H$ $\delta_H$ = 9.9 ppm.[26] The signal at 32 ppm is (i) the only one observed in **1-$_{75}$**, (ii) the most intense Hf−H resonance in **1-$_{100}$**, (iii) still present in **1-$_{150}$**, and (iv) not observed in **1-$_{250}$**. The variations with respect to temperature of

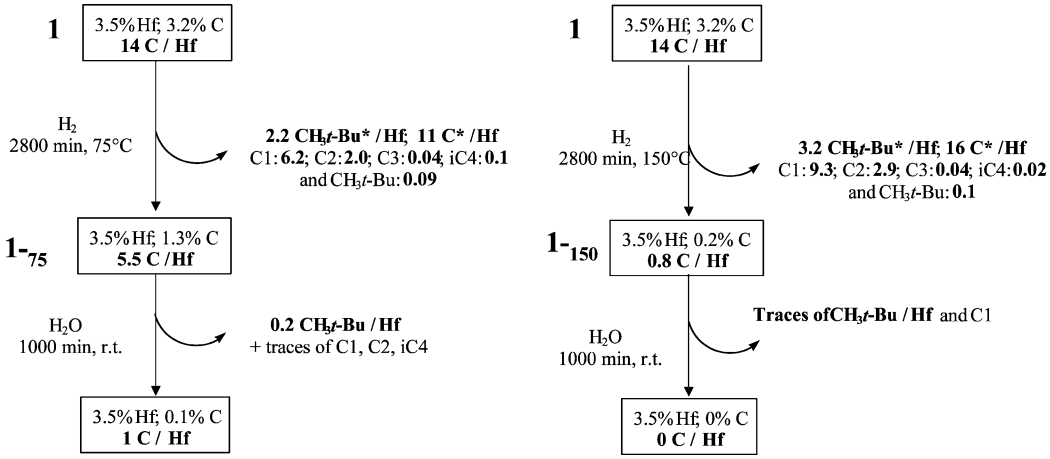


**Figure 5.** Elemental analysis and amount of gas equivalents per mole of grafted hafnium produced during the hydrogenolysis of **1** and the hydrolysis of **1-$_\theta$** ($\theta$ = 75, 150 °C).

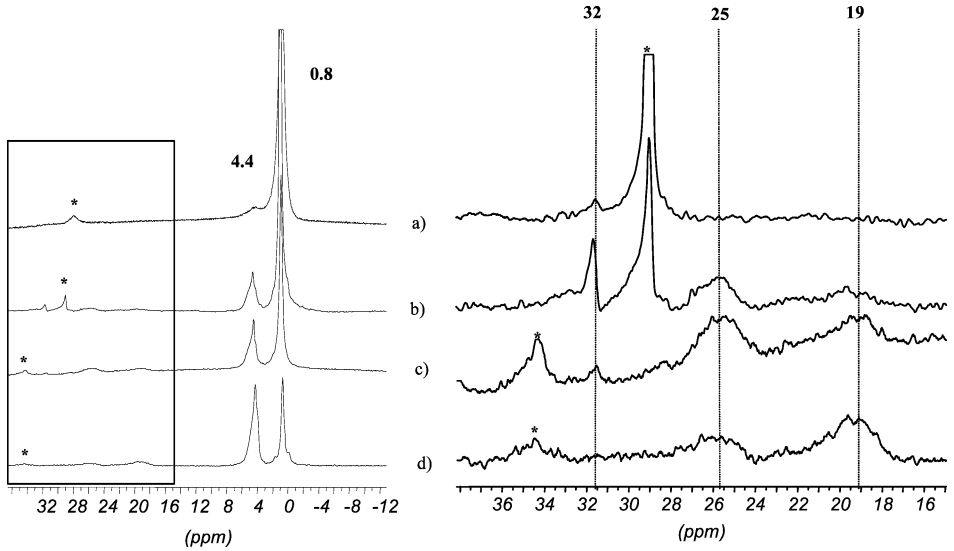


**Figure 6.** (a) 500 MHz $^1$H 10 kHz solid-state NMR spectrum of $\mathbf{1}_{-75}$, (b) 500 MHz $^1$H 10 kHz solid-state NMR spectrum of $\mathbf{1}_{-100}$, (c) 300 MHz $^1$H 10 kHz solid-state NMR spectrum of $\mathbf{1}-_{150}$, and (d) 300 MHz $^1$H 10 kHz solid-state NMR spectrum of $\mathbf{1}$-$_{250}$. *Spinning side bands.

the intensity of the resonance at 32 ppm and of the $\nu_{(Hf-H)}$ bands at 1651 and 1685 cm$^{-1}$ are identical, so consequently, the $\delta^1_H$ at 32 ppm is attributed to **2**.

The broad resonance at 25 ± 0.5 ppm (i) appears in **1**-$_{100}$, (ii) is the most intense peak in **1**-$_{150}$, and (iii) is still present in **1**-$_{250}$. For the same reason as above, this peak is attributed to **3**.

The resonance at 19 ± 0.5 ppm that (i) appears in **1**-$_{100}$ and (ii) is the most intense peak in **1**-$_{250}$ is ascribed to **4**.

To further assign these various signals, double-quanta (DQ) proton spectroscopy under magic angle spinning (MAS) has been performed on **1**-$_{150}$.[8]

Multiquantum proton spectroscopies under fast MAS have been recently shown to be powerful techniques in probing structural information and dynamics inherent to proton−proton dipolar couplings. These techniques have been successfully applied to the characterization of hydrogen-bonding structures, $\pi-\pi$ packing arrangements, and defect sites in zeolites.[33]

Among numerous recoupling sequences, we have chosen the homonuclear symmetry-based post-C7 experiment introduced by Levitt et al.,[34] which is robust with respect to chemical shift offset and rf inhomogeneity[35] and has been extensively used with good efficiency on numerous nuclei including protons.[36]

In this experiment, correlations are observed between pairs of dipolar-coupled protons. The DQ frequency in the $\omega_1$ dimension corresponds to the sum of the two single quantum frequencies of the two coupled protons and correlates in the $\omega_2$ dimension with the two corresponding proton resonances. The observation of a DQ peak implies a close proximity between the two protons involved in this correlation.

Figure 7 shows the $^1$H DQ MAS spectrum recorded for **1**-$_{150}$ at a MAS frequency of 10 kHz using the post-C7 recoupling method (see the Experimental Section for more details).

The $^1$H DQ MAS spectrum of **1**-$_{150}$ (Figure 7) shows a strong autocorrelation peak observed for the proton resonance at 32 ± 0.5 ppm (64 ppm in the $\omega_1$ dimension). This indicates that **2** is a "bis-hydride" complex.

The correlation observed between the broad resonance at 25.5 ± 0.5 ppm (51 ppm in the $\omega_1$ dimension) suggests that **3** is also a hafnium bis-hydride complex in which the two protons have a slightly different chemical shift at 25 ± 0.5 and 26 ± 0.5 ppm due to a different local environment. This is confirmed by the presence of a weaker correlation band between only one of these two proton peaks (the one at 25 ± 0.5 ppm) and the resonance of SiH at 4.5 ± 0.5 ppm (29.5 ± 0.5 ppm in the $\omega_1$ dimension), the weak intensity indicating a longer distance between the two species.

The proton resonance at 19 ± 0.5 ppm does not give any autocorrelation DQ peak at 38 ppm in the $\omega_1$ dimension; this suggests that **4** is a hafnium monohydride. However, the resonance of this proton at 19 ± 0.5 ppm shows a correlation

(24) Zhou, M.; Zhang, L.; Dong, J.; Qin, Q. *J. Am. Chem. Soc.* **2000**, *122*, 10680−10688.
(25) Lokshin, B. V.; Klemenkova, Z. S.; Ezernitskaya, M. G.; Strunkina, L. I.; Brainina, E. M. *J. Organomet. Chem.* **1982**, *235*, 69−75.
(26) Roddick, D. M.; Fryzuk, M. D.; Seidler, P. F.; Hillhouse, G. L.; Bercaw, J. E. *Organometallics* **1985**, *4*, 97−104.
(27) Chertihin, G. V.; Andrews, L. *J. Am. Chem. Soc.* **1995**, *117*, 6402−6403.
(28) Chertihin, G. V.; Andrews, L. *J. Phys. Chem.* **1995**, *99*, 15004−15010.
(29) Cho, H.-G.; Andrews, L. *J. Phys. Chem. A* **2004**, *108*, 10441−10447.
(30) Balasubramanian, K.; Das, K. K. *J. Mol. Spectrosc.* **1991**, *145*, 142−150.
(31) Campbell-Ferguson, H. J.; Ebsworth, E. A. V.; MacDiarmid, A. G.; Yoshioka, T. *J. Phys. Chem.* **1967**, *71*, 723−726.
(32) Silverstein, R. M.; Bassler, G. C.; Morill, T. C. *Spectrometric Identification of Organic Compounds*, 4th ed. ed.; Wiley: New York, 1992.
(33) (a) Geen, H.; Titman, J. J.; Gottwald, J.; Spiess, H. W. *Chem. Phys. Lett.* **1994**, *227*, 79. (b) Geen, H.; Titman, J. J.; Gottwald, J.; Spiess, H. W. *J. Magn. Reson., Ser. A* **1995**, *114*, 264. (c) Friedrich, U.; Schnell, I.; Demco, D. E.; Spiess, H. W. *Chem. Phys. Lett.* **1998**, *285*, 49. (d) Schnell, I.; Brown, S. P.; Low, H. Y.; Ishida, H.; Spiess, H. W. *J. Am. Chem. Soc.* **1998**, *120*, 11784. (e) Brown, S. P.; Spiess, H. W. *Chem. Rev.* **2001**, *101*, 4125. (f) Brown, S. P.; Zhu, X. X.; Saalwaechter, K.; Spiess, H. W. *J. Am. Chem. Soc.* **2001**, *123*, 4275. (g) Brown, S. P.; Schnell, I.; Brand, J. D.; Muellen, K.; Spiess, H. W. *J. Am. Chem. Soc.* **1999**, *121*, 6712. (h) Brown, S. P.; Schaller, T.; Seelbach, U. P.; Koziol, F.; Ochsenfeld, C.; Klarner, F.-G.; Spiess, H. W. *Angew. Chem., Int. Ed.* **2001**, *40*, 717. (i) Shantz, D. F.; Schmedt auf der Guenne, J.; Koller, H.; Lobo, R. F. *J. Am. Chem. Soc.* **2000**, *122*, 6659.
(34) Hohwy, M.; Jakobsen, H. J.; Eden, M.; Levitt, M. H.; Nielsen, N. C. *J. Chem. Phys.* **1998**, *108*, 2686−2694.
(35) Karlsson, T.; Popham, J. M.; Long, J. R.; Oyler, N.; Drobny, G. P. *J. Am. Chem. Soc.* **2003**, *125*, 7394−7407.
(36) Brown, S. P.; Lesage, A.; Elena, B.; Emsley, L. *J. Am. Chem. Soc.* **2004**, *126*, 13230−13231.

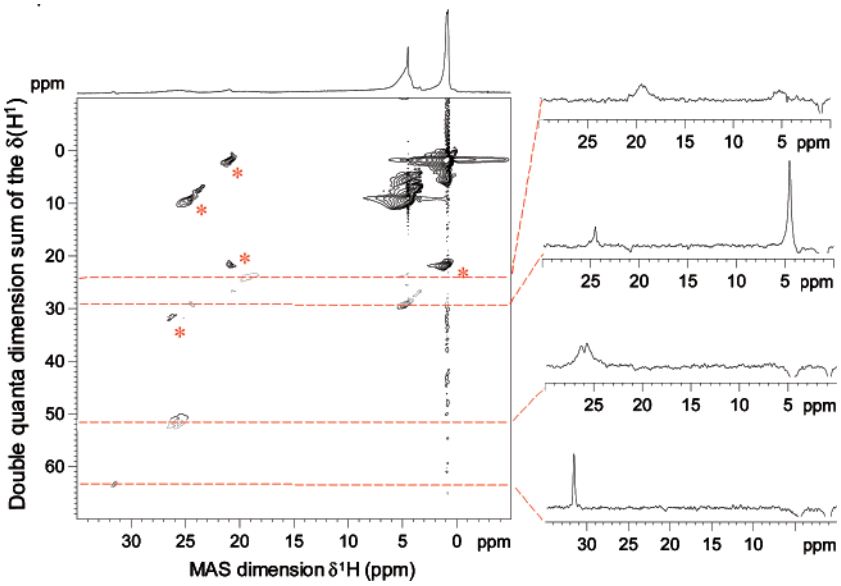


**Figure 7.** $^1$H DQ MAS spectrum recorded for **1**$-_{150}$.

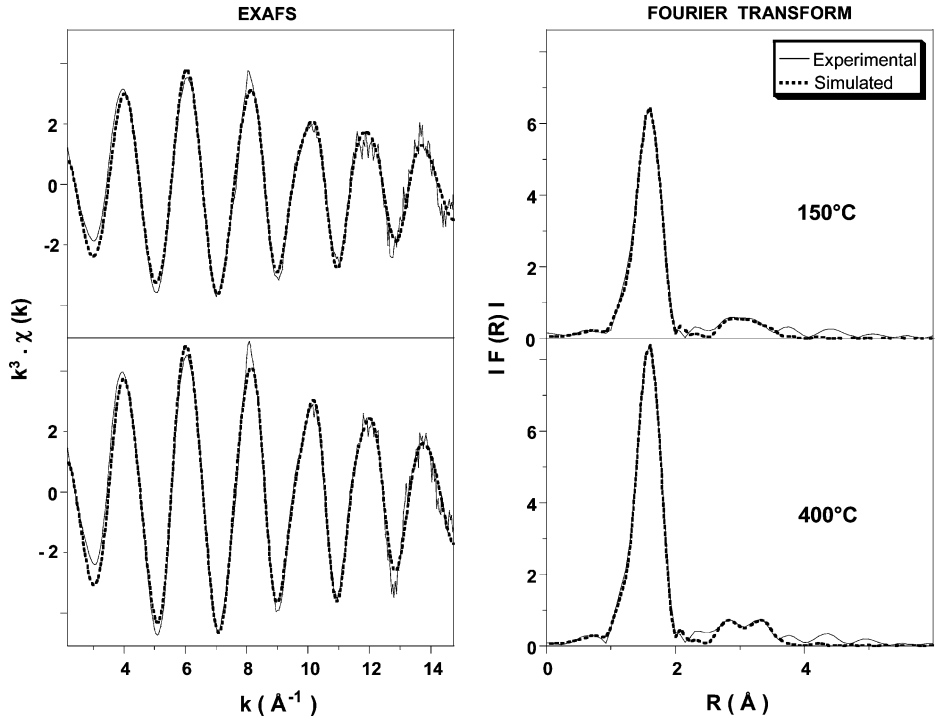


**Figure 8.** $k^3$-Weighted EXAFS at the Hf $L_{III}$-edge (left) and corresponding Fourier transforms (right) with comparison to simulated curves for $(\equiv SiO)_nHfH_{4-n}$ species synthesized on $SiO_{2-(800)}$ and prepared from $\equiv SiO-Hf(CH_2tBu)_3$ at 150 or 400 °C. Solid lines: experimental; dashed lines: spherical wave theory.

with the SiH resonance at 5.5 ± 0.5 ppm (24.5 ± 0.5 ppm in the $\omega_1$ dimension).

In the literature, $\delta$(SiH) is situated upfield compared to $\delta(SiH_2)$ [$(EtO)_3SiH$, $\delta(H) = 4.09$ ppm, $(EtO)_2SiH_2$, $\delta(H) = 4.42$ ppm].[31] By comparison, we can attribute the resonance at 4.5 ± 0.5 ppm to the resonance of [$(\equiv SiO)_3SiH$] and the one at 5.5 ± 0.5 ppm to the resonance of [$(\equiv SiO)_2SiH_2$]. Therefore, the resonance of **4** at 19 ± 0.5 ppm correlates with the resonance of the silicon bis-hydride [$(\equiv SiO)_2SiH_2$], and the resonance of **3** at 25 ± 0.5 ppm with the resonance of the silicon mono-hydride [$(\equiv SiO)_3SiH$].

These data demonstrate that the hafnium bis-hydride **3** is in the vicinity of [$(\equiv SiO)_3SiH$] and that the hafnium mono-hydride **4** is close to [$(\equiv SiO)_2SiH_2$].

As expected, strong autocorrelation peaks are observed for the alkyl (1.6 ppm in the $\omega_1$ dimension) and for the [$(\equiv SiO)_2SiH_2$] proton resonances (9 ppm in the $\omega_1$ dimension).

**EXAFS Results.** The structures of **4** and **5** were also investigated by EXAFS spectroscopy at the hafnium $L_{III}$ edge. Figure 8 shows the experimental and fitted EXAFS signals. For **4**, the fit corresponds to a first coordination sphere of ca. three oxygen atoms at 1.943(4) Å coordinated to hafnium, which can be attributed to three $\sigma$-bonded siloxy ligands ($-\boldsymbol{O}Si\equiv$). Indeed, this bond length is similar to the values obtained from X-ray crystallographic studies for Hf−O distances in hafnium complexes containing silsesquioxane, siloxy, or hydroxy groups, i.e., $Cp_2Hf(c\text{-}C_5H_9)_7Si_7O_{11}(OSiMe_2R)$ (1.97 Å),[38] $Hf[OSi(OtBu)_3]_4$, $Hf[OSi(OtBu)_3]_4(H_2O)$ (1.912−1.929 Å), and $Hf(OH)_4$ (1.939

**Scheme 1. Possible Mechanism of Formation of the Surface Complex [≡SiO−Hf(CH$_2$*t*Bu)H$_2$], 2, from [≡SiO−Hf(CH$_2$*t*Bu)$_3$], 1**

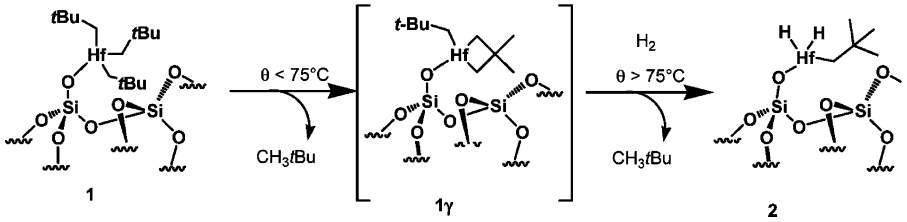


**Scheme 2. Evolution with the Temperature of [≡SiO−Hf(CH$_2$*t*Bu)H$_2$], 2, into [(≡SiO)$_2$HfH$_2$], 3, with Concomitant Formation of Silicon Monohydride, ≡SiH**

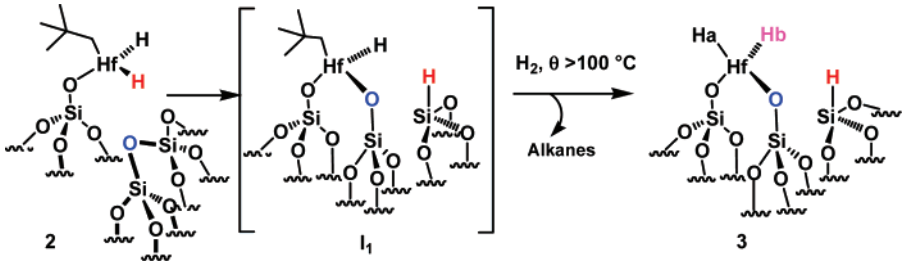


**Table 1. Correlation between IR and Solid-State $^1$H NMR Data**

| IR frequencies $\nu_{(HfH)}$ (cm$^{-1}$) | solid-state NMR $^1$H chemical shift $\delta$(HfH) (ppm) | attribution |
|---|---|---|
| 1651, 1685 cm$^{-1}$ | 32 | **2** |
| 1675, 1720 cm$^{-1}$ | 25 | **3** |
| 1701 cm$^{-1}$ | 19 | **4** |

Å).[39,40] The surface species **1** has already been studied by EXAFS spectroscopy.[19] The spectrum of **1** corresponds to a coordination sphere of two resolved contributions of light atoms at ca. 1.95 and 2.19 Å. While the first contribution was assigned to ca. one O atom at 1.947(7) Å, the second was attributed to three C atoms at 2.191(7) Å, a distance that is similar to the one we found by EXAFS for $HfNp_4$ in benzene (2.19(1) Å), our reference sample. This Hf−C distance is also consistent, though slightly shorter, with the corresponding bond distances reported for analogous molecular complexes.[41] So, due to this significant difference in length between Hf−C and Hf−O bonds, we can assign the light atoms at ca. 1.95 Å to oxygen atoms.

Additional shells could be tentatively added to improve the fit, since they decreased the quality factor from 1.40 to 1.29 for **4**. One shell includes ca. three nonbonding silicons at 3.37(4) Å, which may correspond to the silicon atoms of (≡*Si*O−Hf) moieties, and two other shells are composed of oxygen atoms at 3.38(4) and 3.72(4) Å, which may correspond to siloxy groups, ≡Si*O*Si≡, of the silica surface. The EXAFS-derived parameters are collected in Table 2. With a $k^1$ weighting the results of the fit were very similar. For **5**, the results are very similar concerning the distances of each shell but differ mainly in the number of neighbors in the two first shells (Table 2). A first coordination sphere of ca. four oxygen atoms at 1.940(3) Å coordinated to hafnium can be attributed to four $\sigma$-bonded siloxy groups (−***O***Si≡), and the inclusion of three additional shells reduces the quality factor from 1.95 to 1.72. In conclusion, the results of the analyses of the EXAFS data agree very well

**Table 2. Hf L$_{III}$-Edge EXAFS-Derived Structural Parameters ($k^3$ weighting) for (≡SiO)$_n$HfH$_{4-n}$ Species Synthesized on SiO$_{2-(800)}$ and Prepared from ≡SiO−Hf(CH$_2$*t*Bu)$_3$ under Hydrogen at 150 and 400 °C (single scattering theory; values in parentheses represent the errors generated in RoundMidnight)**

| scatterer | no. of neighbors | distance from Hf (Å) | D.W. factor ($\sigma^2$, Å$^2$) |
|---|---|---|---|
| (≡SiO)$_n$HfH$_{4-n}$ Species Prepared at 150 °C[a] | | | |
| Hf−*O* | 3.0(2) | 1.943(4) | 0.0032(4) |
| Hf···*Si* | 2.6(12) | 3.37(4) | 0.014(10) |
| Hf···*O*′Si$_2$ | 2.3(10) | 3.38(4) | 0.004(2) |
| Hf···*O*″Si$_2$ | 0.8(5) | 3.72(4) | 0.004[b] |
| (≡SiO)$_n$HfH$_{4-n}$ Species Prepared at 400 °C[a] | | | |
| Hf−*O* | 3.8(3) | 1.940(3) | 0.0030(3) |
| Hf···*Si* | 3.6(14) | 3.39(3) | 0.015(9) |
| Hf···*O*′Si$_2$ | 2.2(9) | 3.40(2) | 0.003(2) |
| Hf···*O*″Si$_2$ | 1.1(5) | 3.73(3) | 0.003[b] |

[a] Fit residue: $\rho = 2.8\%$ ($\Delta k = 2.2-14.8$ Å$^{-1}$, $\Delta R = 0.6-3.6$ Å); energy shift: $\Delta E_0 = 7.1(6)$ eV, the same for all shells; overall scale factor: $S_0^2 = 0.98$; number of parameters fitted: $P = 12$; number of degrees of freedom in the fit: $\nu = 14$; quality factor of the fit: $(\Delta\chi)^2/\nu = 1.29$. [b]Shell constrained to the parameter above. [c]Fit residue: $\rho = 2.2\%$ ($\Delta k = 3.2-14.8$ Å$^{-1}$, $\Delta R = 0.6-3.6$ Å); energy shift: $\Delta E_0 = 7.1(5)$ eV, the same for all shells; overall scale factor: $S_0^2 = 0.98$; number of parameters fitted: $P = 12$; number of degrees of freedom in the fit: $\nu = 14$; quality factor of the fit: $(\Delta\chi)^2/\nu = 1.72$.

with the following structures proposed for the surface complexes: (≡SiO)$_3$Hf−H for **4** and (≡SiO)$_4$Hf for **5**.

## Discussion

All analyses realized on samples of **1**-$_\theta$, $\theta$ = 75 100, 125, 150, and 250 °C, are consistent with the formation of three supported hafnium hydride complexes: **2**, **3**, and **4**. With increasing temperature, the evolution of **2** into **3** and **4** can occur through two routes, both involving the opening of a siloxane bridge [≡Si−O−Si≡]. The first route produces **3** with concomitant

(37) Mortensen, J. J.; Parrinello, M. J. *Phys. Chem. B* **2000**, *104*, 2901−2907.
(38) Wada, K.; Itayama, N.; Watanabe, N.; Bundo, M.; Kondo, T.; Mitsudo, T.-a. *Organometallics* **2004**, *23*, 5824−5832.
(39) Terry, K. W.; Lugmair, C. G.; Tilley, T. D. *J. Am. Chem. Soc.* **1997**, *119*, 9745−9756.
(40) Lugmair, C. G.; Tilley, T. D. *Inorg. Chem.* **1998**, *37*, 764−769. Wang, X.; Andrews, L. *Inorg. Chem.* **2005**, *44*, 7189−7193.
(41) (a) Liang, L.-C.; Schrock, R. R.; Davis, W. M. *Organometallics* **2000**, *19*, 2526−2531. (b) Guo, Z.; Swenson, D. C.; Jordan, R. F. *Organometallics* **1994**, *13*, 1424−1432. (c) Schrock, R. R.; Adamchuk, J.; Ruhland, K.; Lopez, L. P. H. *Organometallics* **2005**, *24*, 857−866. (d) Fryzuk, M. D.; Corkin, J. R.; Patrick, B. O. *Can. J. Chem.* **2003**, *81*, 1376−1387.

**Scheme 3. Evolution with the Temperature of [(≡SiO)$_2$HfH$_2$], 3, into[(≡SiO)$_3$HfH], 4, with Concomitant Formation of Silicon Dihydride (>SiH$_2$)**

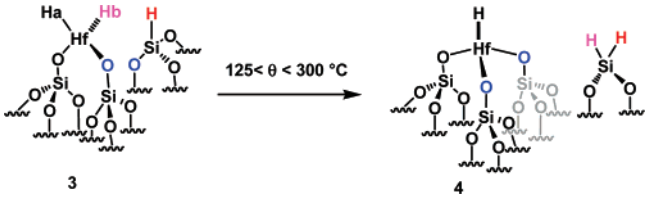


formation of a ≡Si−CH$_2$*t*Bu bond. However, after hydrolysis of **2**, no more carbon remains present on the surface. Since the ≡Si−CH$_2$*t*Bu bond is not expected to be water-sensitive and since this step does not generate $C_1$ and $C_4$, this route is less likely. The other route results in the concomitant formation of hafnium hydrides **3** and **4**, [(≡SiO)$_3$SiH], [(≡SiO)$_2$SiH$_2$], and alkanes $C_1$−$C_4$ through siloxane bridge (≡Si−O−Si≡) opening and the hydrogenolysis of a neopentyl ligand.[2,18,21,37]

The infrared spectroscopy and the analytical data of the continuous-flow reactor experiment show that there is *no hydrogenolysis* of **1** *until 75 °C*. Therefore, the neopentane evolved is formed via $\gamma$-H abstraction and reductive elimination.[19] When the temperature reaches 75 °C under hydrogen, **1-$_{75}$**, there are successive cleavages of the Hf−C bond, affording the major surface hydride **2**. **2** is characterized by $\delta_{(HfH)}$ of 32 ppm and $\nu_{(HfH)}$ at 1651 and 1685 cm$^{-1}$. Analytical data from the continuous-flow reactor experiment show that in **1-$_{75}$**, *5 C/Hf* remain on the surface and that they are released by hydrolysis of the solid mainly as neopentane. This means that a Hf−CH$_2$*t*Bu ligand is present on **2**. The strong autocorrelation peak observed at 64 ppm in the $\omega_1$ dimension of the $^1$H DQ MAS spectrum of **1-$_{75}$** means that the resonance at 32 ppm can be assigned to a bis-hydride species.[8] Consequently, in **1-$_{75}$** there is a major surface species, in which the Hf center is linked to one CH$_2$*t*Bu and two hydride ligands: ≡SiO−Hf(CH$_2$*t*Bu)H$_2$], **2**. The data of the experiments carried out at 150 °C, leading to **1-$_{150}$**, prove that there are little to no Hf−C bonds and that two main hydride surfaces, **3** and **4**, coexist on the surface.

**3** is characterized by $\delta_{(HfH)}$ at 25 and 26 ppm and $\nu_{(HfH)}$ at 1675 and 1720 cm$^{-1}$. Since there is an autocorrelation peak for this resonance in the $^1$H DQ MAS spectrum (51 ppm in the $\omega_1$ dimension), **3** is a bis-hydride species. The fact that two peaks are observed in the $\omega_2$ dimension and that only the resonance at 25 ppm is correlated with the resonance $\delta$(≡SiH) indicate that in **3** the two hydrides bonded to the Hf are in a different local environment. At this point, all the experimental data suggest that **3** is [(≡SiO)$_2$HfH$_2$], and that is close to [(≡SiO)$_3$SiH]. As the $^1$H DQ MAS spectrum proves that the two protons are nonequivalent (26 and 25 ppm) and that only the resonance at 25 ppm is correlated with the resonance $\delta$(≡SiH), the local structure of **3** is that shown in Scheme 2.

**4** is characterized by $\nu_{(HfH)}$ at 1701 cm$^{-1}$ and $\delta_{(HfH)}$ at 19 ppm, which does not give an autocorrelation DQ peak at 38 ppm in the $\omega_1$ dimension in the $^1$H DQ MAS spectrum. It shows a weak correlation with the [(≡SiO)$_2$SiH$_2$ ] resonance (24 ppm in the $\omega_1$ dimension).[8] The structure of **4** is therefore [(≡SiO)$_3$HfH] and is close to [(≡SiO)$_2$SiH$_2$].

At the beginning, in our experimental conditions **3** and **4** seem to form at more or less the same time and **4** is possibly faster. However the $^1$H DQ MAS data are consistent with the concomitant formation of **3** and [(≡SiO)$_3$SiH] and of **4** and [(≡SiO)$_2$SiH$_2$]

Moreover, up to 150 °C the amount of **3** and **4** decrease, but the amount of **4** decreases less rapidly than **3**. In contrast, the amount of [(≡SiO)$_3$SiH] and [(≡SiO)$_2$Si(H)$_2$] increase. Consequently, the formation of **4** could result from the reaction of **3** with another siloxane bridge [≡Si−O−Si≡], yielding **4** with concomitant formation of [(≡SiO)$_2$SiH$_2$].

The evolution of **3** into **4** is total when the temperature reaches 300 °C, Scheme 3.

Then, at 400 °C, the intensity of vibrations $\nu_{(HfH)}$ is equal to zero: **4** is transformed into a tetrasiloxy surface species [(≡SiO)$_4$Hf)], **5**, with simultaneous formation of [(≡SiO)$_3$SiH]. All the analytical and spectral data correspond and suggest that **2**, **3**, and **4** are formed consecutively and the formation of **3** and [(≡SiO)$_3$SiH] and **4** and [(≡SiO)$_2$SiH$_2$] are respectively correlated.

From 300 °C, the intensity of the band due to $\nu_{(SiH2)}$ decreases sharply to zero, whereas the band due to $\nu_{(SiH)}$ increases. Consequently, between 300 and 400 °C, there is total conversion

**Scheme 4. Evolution with the Temperature of [(≡SiO)$_3$HfH], 4, into [(≡SiO)$_4$Hf], 5, and of (>SiH$_2$) into ≡SiH**

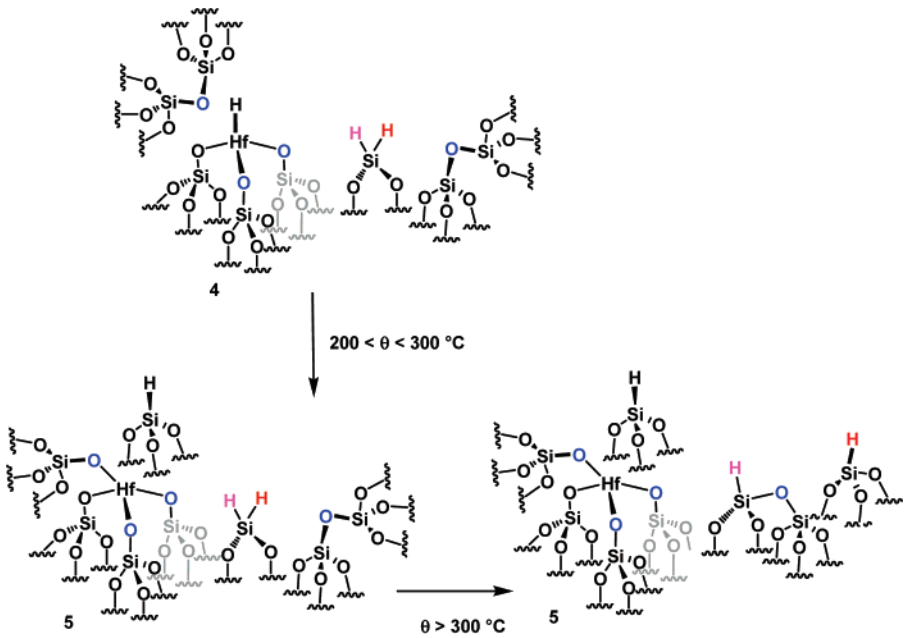

**Scheme 5. Reaction of [≡SiO−Hf($CH_2$$^t$Bu)$_3$], 1, with $H_2$ as a Function of the Temperature Reaction**

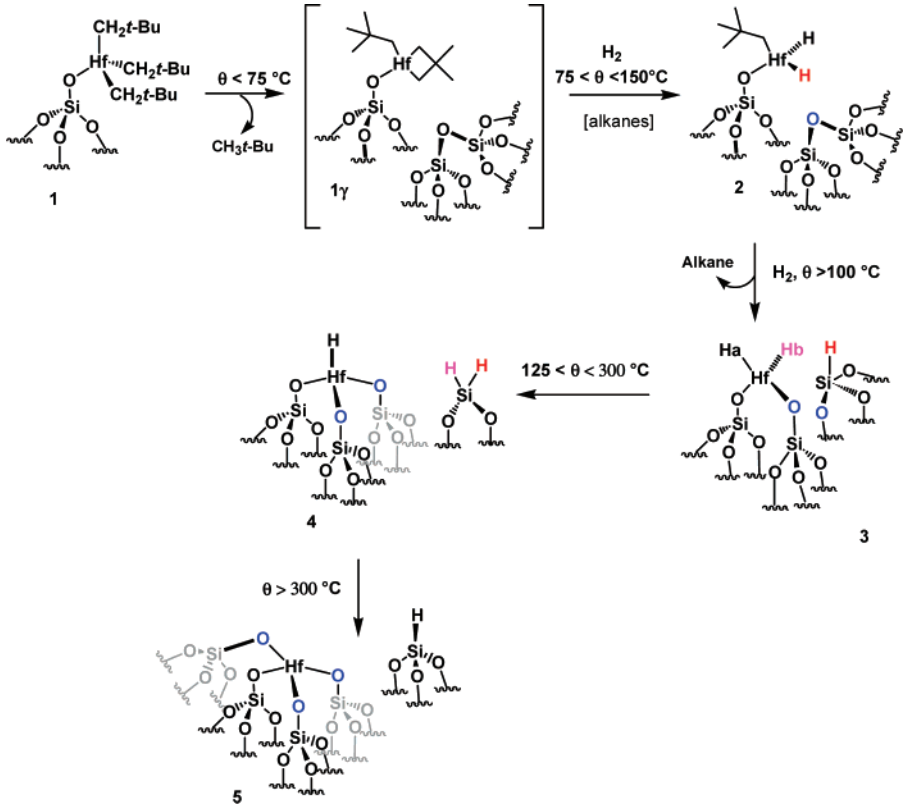


of [(≡SiO)$_2$SiH$_2$] into [(≡SiO)$_3$SiH] (Figure 4). The latter is the only hydride surface species at temperatures above 400 °C.

Even if these hafnium hydrides are thermally very stable, above a certain temperature (300−400 °C) they decompose by reacting with the adjacent siloxy bridges. It is certainly a mode of aging of the catalyst used for hydrogenolysis. Silica can accept the hydrides by a $\sigma$-bond metathesis process, for which the Hf−O−Si bond becomes thermodynamically more stable than the Si−O−Si bond.

## Conclusion

The evolution of **1** under dihydrogen with increasing temperature has been evidenced by several physical and analytical techniques. All surface hydrides have been identified and relatively well characterized. The nature and amount of hafnium hydrides **2**−**5**, [(≡SiO)$_2$SiH$_2$], and [(≡SiO)$_3$SiH] are tunable following the temperature of hydrogenolysis of **1** (Scheme 5). Obviously, hafnium hydrides are thermally quite stable at high temperature, a phenomenon characteristic of surface organometallic chemistry. The reason for such stability is the impossibility of bimolecular recombination and the absence of ligand with which the hydrides could react. Such thermal stability opens a new area for catalysis, as molecular catalysis is not able to work with hydrides at such high temperature.

## Experimental Part

**General Procedures.** All experiments were carried out by using standard air-free methodology in an argon-filled Vacuum Atmospheres glovebox, on a Schlenk line, or in a Schlenk-type apparatus interfaced to a high-vacuum line ($10^{-5}$ Torr). Hydrogen was dried over a deoxo catalyst (BASF R3-11 + 4 Å molecular sieves) prior to use.

Gas-phase analyses were performed on a Hewlett-Packard 5890 series II gas chromatograph equipped with a flame ionization detector and KCl/$Al_2O_3$ on a fused silica column (50 × 0.32 mm).

Elemental analyses were performed at the CNRS Central Analysis Department of Solaize or at the LSEO of Dijon.

Infrared spectra were recorded on a Nicolet 550-FT spectrometer by using a custom infrared cell equipped with $CaF_2$ windows, allowing in situ studies. Typically, 16 scans were accumulated for each spectrum (resolution 2 cm$^{-1}$).

NMR spectra were recorded on an Avance 500 or DSX 300 Bruker NMR spectrometer, using a commercial 4 mm CPMAS probe from Bruker. The samples were prepared under argon in a 4 mm zirconia rotor. The sample spinning speed was $\omega_R = 10$ kHz unless otherwise specified.

**Double-Quantum Spectroscopy.** The proton DQ experiments were designed as follows: rf field strength was 70 kHz ($7\omega_R$) during the excitation and reconversion periods, which were chosen equal to 200 $\mu$s (corresponding to 7 post C7 basic elements); 512 increments of 32 scans each were collected with a 4 s recycle delay, which gave a total experiment time of 18 h. Processing was done with a 50 Hz line broadening in both dimensions and one zero filling in the $\omega_1$ dimension.

**Extended X-ray Absorption Fine Structure Spectroscopy (EXAFS).** X-ray absorption spectra were acquired at the SRS of the CCLRC in Daresbury (UK) with beam-line 7.1, at room temperature at the hafnium $L_{III}$ edge, with a double crystal Si(111) monochromator detuned 70% to reduce the higher harmonics of the beam. The spectra were recorded in the transmission mode between 9.4 and 10.4 keV. The two supported Hf samples, **4** and **5**, prepared as stated in the text and studied by solid-state NMR, were stored in break-seal flasks. They were packaged within a nitrogen-filled drybox in a double airtight sample holder equipped with Kapton windows. This type of cell has already been used and proved to be very efficient for air-sensitive compounds such as

$\equiv SiO-HfNp_3$ species supported on aerosil silica$_{(800)}$, where the Hf−C contribution could be clearly distinguished from Hf−O by EXAFS.[19] The spectra analyzed were the results of four such acquisitions, and no evolution could be observed between the first and last acquisition. The data analyses were performed by standard procedures using the programs developed by Alain Michalowicz, in particular the EXAFS fitting program "RoundMidnight 2005".[42a]

The program FEFF8 was used to calculate theoretical files for phases and amplitudes based on model clusters of atoms.[42b] The value of the scale factor, $S_0^2 = 0.98$, was determined from the spectrum of the reference compound, a benzene solution of $HfNp_4$ (four carbon atoms at 2.19(1) Å in the first coordination sphere). The refinements were performed by fitting the structural parameters $N_i$, $R_i$, $\sigma_i$, and the energy shift, $\Delta E_0$ (the same for all shells). The fit residue, $\rho$ (%), was calculated by the following formula:

$$\rho = \frac{\sum_k [k^3\chi_{exp}(k) - k^3\chi_{cal}(k)]^2}{\sum_k [k^3\chi_{exp}(k)]^2} \times 100$$

As recommended by the Standards and Criteria Committee of the International EXAFS Society,[43] an improvement of the fit took into account the number of fitted parameters (decrease of the quality factor, $(\Delta\chi)^2/\nu$, where $\nu$ is the number of degrees of freedom in the signal).

**Monitoring the Hydrogenolysis of Hf(CH$_2$*t*Bu)$_4$/SiO$_{2-(\theta)}$ by Infrared Spectroscopy.** Silica (15−35 mg) was pressed into a 18 mm self-supporting disk, adjusted in a sample holder, and introduced into a glass reactor equipped with $CaF_2$ windows. Silica was calcined under air at 200 or 500 °C and partially dehydroxylated at the desired temperature. The molecular complex [Hf(CH$_2$*t*Bu)$_4$] was sublimed under dynamic vacuum at 70 °C onto the oxide disk, and the solid was heated at 70 °C for 1 h. The excess of [Hf(CH$_2$*t*Bu)$_4$] was removed by reverse sublimation at 70 °C and condensed into a tube cooled by liquid nitrogen, which was then sealed off using a torch. Hydrogen (500 Torr) was introduced in the cell, and the system was heated to the desired temperature with a temperature slope of 1 °C·min$^{-1}$ and maintained constant for at least 4 h. An infrared spectrum was recorded at each step.

**Hydrogenolysis of Hf(CH$_2$*t*Bu)$_4$/SiO$_{2-(800)}$ in a Continuous-Flow Fixed-Bed Tubular Reactor.** Hf(CH$_2$*t*Bu)$_4$/SiO$_{2-(800)}$ (ca. 300 mg) was loaded under argon in a continuous-flow fixed-bed tubular reactor. The sample was flushed with hydrogen (flow rate of 3.1 mL) for 200 min at room temperature, then heated at a rate of 10 °C·h$^{-1}$ from room temperature to the desired temperature (75 or 150 °C). The temperature was carefully recorded as a function of time, and the composition of evolved gas was determined online by gas chromatography.

**Hydrogenolysis of Hf(CH$_2$*t*Bu)$_4$/SiO$_{2-(\theta)}$ in a Batch Reactor.** The molecular complex grafted onto oxide was introduced in a reactor of known volume under strict exclusion of air. After evacuation of argon, 500 Torr of hydrogen was introduced. The system was heated for 17 or 21 h at the chosen temperature, then the gas phase was analyzed by chromatography.

**Hydrolysis.** The solid (ca. 50 mg) was introduced in a reactor of known volume under strict exclusion of air. After evacuation of argon, the vapor pressure of water was introduced. The reaction was monitored by chromatographic analysis of the gas phase.

**Acknowledgment.** We are grateful to Region Rhône-Alpes for financial support (G.T.) and to Society CEZUS for the samples of $HfCl_4$. The EXAFS data were recorded at the SRS of the CCLRC, in Daresbury, UK (project 44204), at beam line 7.1.

**Supporting Information Available:** This material is available free of charge via the Internet at http://pubs.acs.org.

OM070214Q

(42) (a) Michalowicz, A. *Logiciels pour la chimie*; Société Française de Chimie, 1991; p 102, and personal communications, new programs downloadable at http://www.univ-paris12.fr/lps2m. (b) Ankudinov, A. L.; Ravel, B.; Rehr, J. J.; Conradson, S. D. *Phys. Rev. B: Condens. Matter Mater. Phys.* **1998**, *58*, 7565−7576.

(43) Reports of the Standards and Criteria Committee of the International XAFS Society; http://ixs.iit.edu/subcommittee_reports/sc/, 2000; No. 70, Vol. 70.